

Effect of load and thickness on the constrained sintering of LTCC substrates

Jung-Hwan Cho^a, Dong-Hun Yeo^{a,*}, Hyo-Soon Shin^a, Youn-Woo Hong^a and Sahn Nahm^b

^aFuture Convergence Ceramic Division, Korea Institute of Ceramic Engineering and Technology, Seoul, 153-801, Korea

^bDepartment of Materials Science and Engineering, Korea University, Seoul, 136-701, Korea

It is necessary to develop the technique of high integrity ceramic modules with fine patterning, via hole minimizing, and via hole aligning between the layers. The shrinkage of ceramic bodies during sintering reduces the precision of patterns, via-hole alignments, and the large formatting of the substrates. Therefore the importance of shrinkage control of ceramic substrates during sintering is being increased for fabricating high integration modules using the large and flat multilayer ceramic substrates. In this study, the x-y shrinkage of LTCC substrates was controlled to under 0.2% using alumina sacrificial layers by less-pressure assisted sintering. The laminated sheets of alumina/LTCC/alumina were sintered at 900 °C for 30 minutes in air according to a specified sintering profile. Samples with different thicknesses of LTCC sheet and the alumina layer were sintered and the sintering shrinkage of the x-y and z axis were compared with the radius of edge curvature of them. Also the radii of edge curvature of sintered samples were measured as a function of the loads in the range of zero to 1000 g/cm².

Key words: LTCC, Constrained Sintering, Shrinkage, Alumina/LTCC/alumina.

Introduction

LTCC technology has many advantages such as low dielectric loss, low cost, and high reliability in the high fully embedded within a multi-layered module or substrate and other discrete components or modules can be mounted on these surfaces of the embedded substrates space-efficiently [1, 2].

The non-uniform shrinkage during firing generally makes a camber or warpage in laminated ceramics and a tolerance of 0.5% in the x-y shrinkage, which is in the range of 12-18%, makes the inter-layer misalignment between the patterns and via holes. In order to reduce the dimensional uncertainty of ceramic substrates during the firing process, various zero shrinkage methods[3-5] have been used in industry to try to solve, reduce or avoid the shrinkage problem. The pressure assisted sintering (PAS) method has been used to manufacture multi-layered ceramic substrates due to its simple feasibility. Green multi-layered ceramic substrates are pressed to the z direction during firing [6, 7]. This method needs special equipment which press the substrate to be sintered uniaxially from both sides of the top and bottom. The pressure inhibits the shrinkage along the x-y directions and promotes that along the z direction. As in the pressure-less assisted sintering (PLAS) method, the stacked LTCC layers are placed between two constrained layers which have a high sintering temperature [8]. Also the thicker the LTCC layer with a high integrity, the more the curvature occurs at the

edge lines of the substrate. And this curvature causes the mis-alignment of the patterns and via holes [9].

To solve the various problems in these methods, we suggest a less pressure assisted sintering (L-PAS) process with a constrained layer in this study. This method would make it possible to obtain a large working area of the LTCC substrate with the precise alignment among many LTCC layers. In addition, this method does not require extra equipment. In this method, the LTCC layers are placed between the constrained layers and a thick plate which is thermally stable at the sintering temperature and has a certain weight loaded on top of the constrained layer.

In this study, the relationship between the thickness of the LTCC and the loaded weight for the L-PAS method will be investigated, and also the edge curvature will be controlled through a control of the shrinkage during sintering.

Experimental Procedure

Commercial alumina powder (AES-11, Sumitomo, Japan) was used for the constrained layers and commercial LTCC powder (MLS-22C, Nippon Electric Glass, Japan) was used for the substrate. The properties of the two powders are shown are in table 1.

Both the alumina powder and the LTCC powder were

Table 1. Properties of commercial raw materials

	Density (g/cm ³)	Particle size D ₅₀ (μm)	Crystal structure	Composition
LTCC (MLS-22C)	3.2	2.6	Anorthite	Al ₂ O ₃ filler + Ca-Al-Si-O glass
Alumina (AES-11)	3.9	0.5	•-alumina	Al ₂ O ₃

*Corresponding author:
Tel : +82-2-3282-2433
Fax: +82-2-3282-7837
E-mail: ydh7@kicet.re.kr

dispersed in a dispersant solvent by a ball-mill for 24 hours. Then the plasticized binder was mixed with the dispersion of each powder by a ball-mill for extra 24 hours. The milling media was zirconia balls. The mixed slurry of each powder was de-gassed to have a viscosity of 3,000 cps. Each de-gassed slurry was tape-cast into a green sheet. The sheets were laminated into a green substrate one after another at 75 kgf/cm^2 and 60°C for 5 minutes. On the laminated $500 \mu\text{m}$ sheets of the alumina, a bundle of the LTCC sheets was laminated and then other alumina sheets of the same thickness were laminated on that LTCC sheet bundle to make a sandwich structure. The thickness of the single LTCC sheet was $200 \mu\text{m}$. After warm isostatic pressing, the green sheet was cut into a size of $10 \times 10 \text{ mm}$. Cut specimens were fired at 500°C for 2 hours with a heating rate 1 K/min to burn out the organics in the specimens. After binder burn-out, the specimens were fired continuously in the kiln at 900°C for 30 minutes with a heating rate of 5 K/min . Before firing, an additional porous plate was placed on top of the cut specimen, and another as a porous plate was placed beneath the cut specimen. Stainless steel plates with weights from 0 g to 1000 g was loaded on the upper porous plate.

The specimens were also observed by an optical microscope (Icamscope-G, Icamscope, Korea) to measure the shrinkage along both the x-y direction and z direction. The edge curvature was measured and its radius was calculated by a 3-point circle approximation as shown in Fig. 1.

The effect of the amount of load on the shrinkage of the specimens during the sintering were simulated using the computer program (ANSYS, ver. 9.0)

Result and Discussion

Fig. 2 shows the in-situ observations of a symmetric sandwich-structured specimen by a high temperature optical microscope, as fired up to 900°C with a heating rate of 5 K/min . The thickness of the alumina layer was $500 \mu\text{m}$, and that of the LTCC was 2.9 mm . From room temperature (a) to the 500°C , the temperature of binder-burn out (b), there was no deformation observed in specimen. But curvature of specimen occurred at 800°C (c), and was

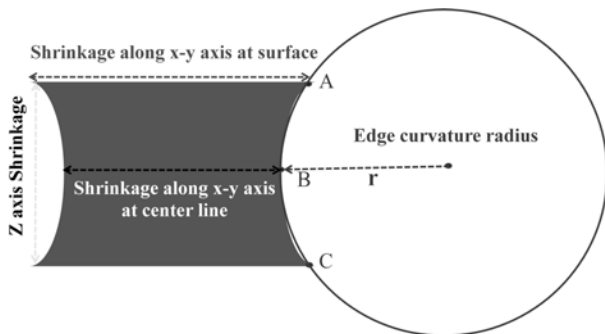


Fig. 1. Evaluation of the edge curvature in the L-PAS method with the measurement of three shrinkage displacement at the surface, center line and edge.

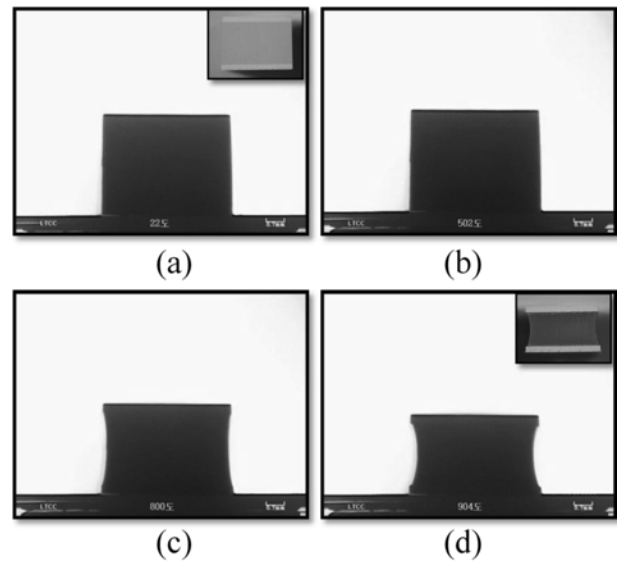


Fig. 2. In situ observations of a sandwich-structured specimen with a high temperature optical microscope as fired up to 900°C . Captured at (a) 20°C , (b) 500°C , (c) 800°C , and (d) 900°C .

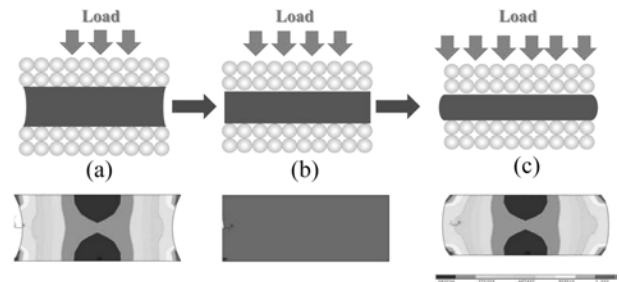


Fig. 3. Computer-aided simulation describing the effect of load in the L-PAS method. With (a) insufficient load, (b) adequate load, (c) excessive load.

maximized at 900°C (d). This implies that the shrinkage difference between the alumina and the LTCC cause the curvature along with a constrained phenomenon [10].

The effect of the load on the shrinkage behavior in the L-PAS method is modeled on Fig. 3. This shows the simulated stress distribution with a variation in load in the L-PAS method. The size of the specimens was set at $10 \times 4 \text{ cm}$, and the shrinkage stress along the x direction was set at 34 kPa . The load in the z direction was varied. In (a) with a stress less than 68 kPa , the load does not compensate the shrinkage difference, so the curvature with a negative radius occurs. The maximum stress occurs at the 'tip' parts of the LTCC and a stress gradient would occur in the LTCC body. With an adequate load as shown in (b), the load seems to compensate sufficiently the lack of the shrinkage difference between the interfacial parts and the interior ones of LTCC so a curvature does not occur. And the shrinkage along the z direction was large shrinkage than that in (a). With an excessive load as shown in (c), the load seems to compensate too much the shrinkage of the LTCC so a positive radius curvature occurs. And the shrinkage along the z direction was the largest among those in (a), (b), and (c). In the simulated results, it can be

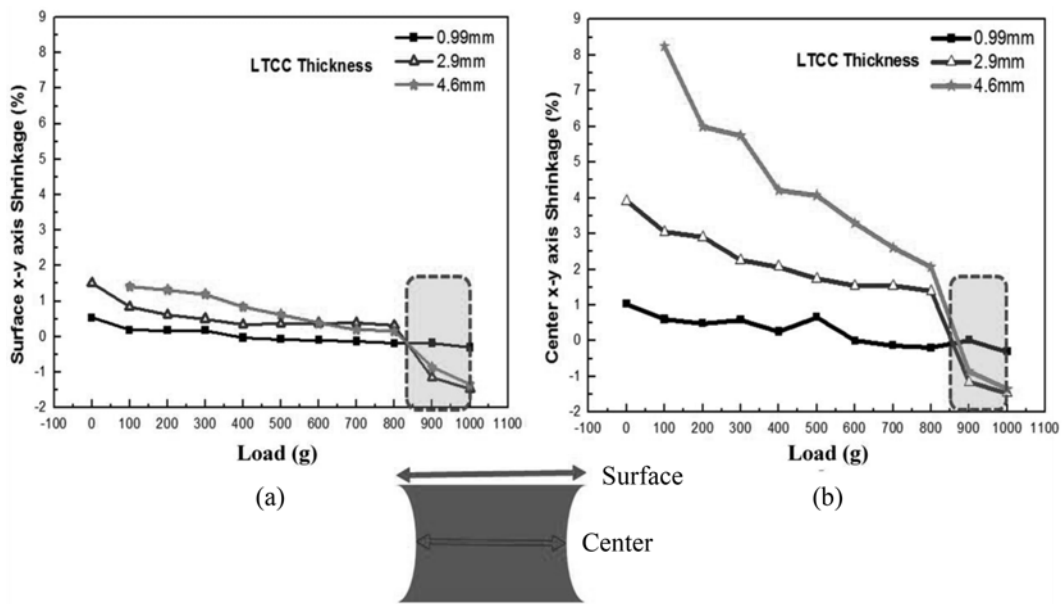


Fig. 4. Effect of the load and the LTCC thickness on the shrinkage along the x-y directions in different parts. (a) at the surface, and (b) at the center line.

thought that an adequate load make the zero-shrinkage substrate with the L-PAS method.

Fig. 4 shows the shrinkage change along the x-y directions with a variation of the load. The alumina thickness was fixed at 500 μm and the chosen LTCC thicknesses were 0.99 mm, 2.9 mm and 4.6 mm. The load was varied from 100 g to 1000 g with a step of 100 g. Fig. 4(a) shows the shrinkage along the x-y directions at the surface, and Fig. 4(b) shows that at the center line. In Fig. 4(a), the shrinkage decreased as the load increased and approached zero at a load of 800 g. With a load of 900 g or more, the shrinkage value was negative for the LTCC thicknesses of 2.9 mm and 4.6 mm. For the LTCC with a thickness of 0.99 mm, there was no noticeable change in the shrinkage. This implies that the shrinkage is more affected by the load as the LTCC thickness is increased. In Fig. 4(b), the decreasing trends of shrinkage are similar with that of Fig. 4(a), but the decrement in the shrinkage was greater than that seen in Fig. 4(a). The thickest LTCC of 4.6 mm showed the largest decrement from 8% at a 100 g load to 2% at a 800 g load. The shrinkage value -1.53% at a 1000 g load is thought to be meaningless, because it is thought to be due to the collapse of the LTCC body. Practically, the shrinkage difference between the surface and the center line was minimized at a 800 g load. But, between 800 g and 900 g, it is thought that there might exist some critical load point where the difference equals zero.

Fig. 5 shows the shrinkage along the x-y directions with a variation of the LTCC layer thickness. For four values of the load 100 g, 400 g, 700 g, 1000 g, the shrinkages were measured. For each relation of the shrinkage versus the thickness, linear lines were drawn. The slopes of these lines decreased with an increase of the load. Even for a load of 1000 g, the slope is negative and it is thought that

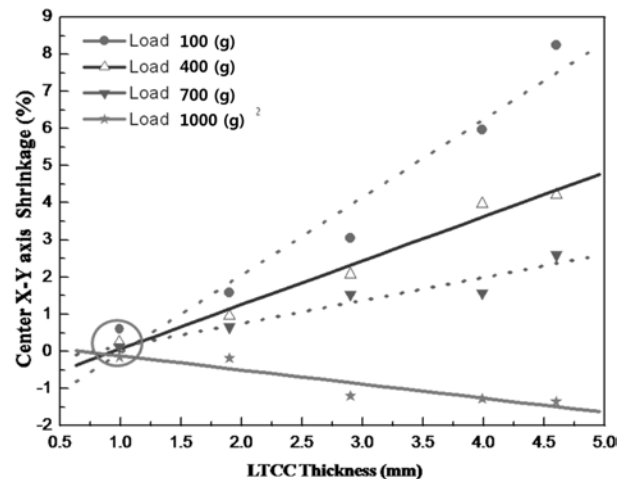


Fig. 5. The effect of the LTCC thickness on the shrinkage along the x-y directions at the center line with loads of 100 g, 400 g, 700 g, and 1,000 g.

the negative slope reflects a deformation of a positive-radius curvature. Between 700 g and 1000 g, there would be some critical load value which has a slope of zero regardless of the LTCC thickness as suggested in Fig. 4. All the fit lines converge at an LTCC thickness of 1.0 mm and this corresponds with a shrinkage near zero, and it could be thought that below a thickness of 1.0 mm a zero-shrinkage substrate could be obtained without a load.

Fig. 6 shows the shrinkage along z direction with a variation of the LTCC layer thickness. For four values of the load 100 g, 400 g, 700 g and 1000 g the shrinkages were measured. In each case, linear fit lines were drawn. The slopes of the fit lines were negative but increased with an increase of the load. They converged below an LTCC

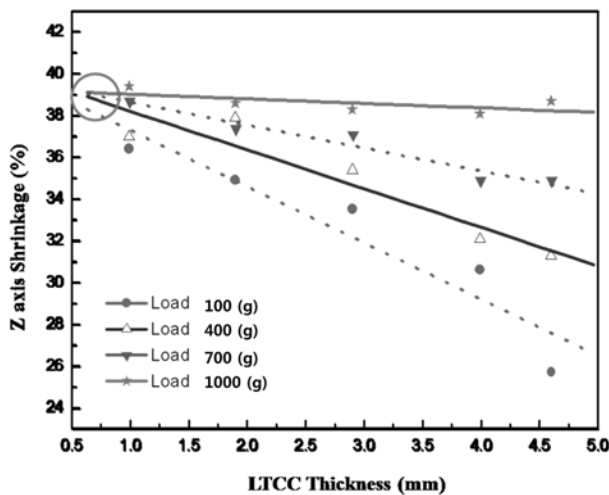


Fig. 6. The effect of the LTCC thickness on the shrinkage along the z direction at the center line with loads of 100 g, 400 g, 700 g, and 1,000 g.

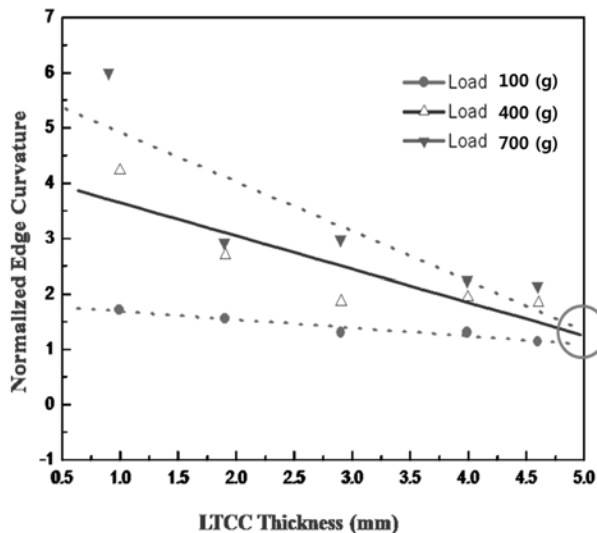


Fig. 7. The effect of the LTCC thickness on the normalized edge curvature along the x-y directions at the center line with loads of 100 g, 400 g, 700 g, and 1,000 g.

thickness of 1.0 mm. Sufficient shrinkage along the z direction indicates that the shrinkage along the x-y directions is sufficiently small. A load value of 1000 g showed a high shrinkage along the z direction regardless of LTCC thickness.

Fig. 7 shows the normalized edge curvatures with a variation of the LTCC layer thickness. For three values of the load 100 g, 400 g, and 700 g, the shrinkages were measured. For each relation of the normalized curvature versus the thickness, linear fit lines were drawn. The slopes of the fit lines were negative and decreased with an increase of the load, in other words the higher the load, the steeper the slopes. Here, the normalized edge curvature was calculated by the following equation:

$$\text{normal edge curvature} = \frac{\text{edge curvature}}{\text{LTCC thickness}} \quad (1)$$

The three fit lines converged above 5.0 mm of LTCC thickness and this implies that above thickness any amount of load could not affect the edge curvature.

From the results of Fig. 5, 6, and 7, the L-PAS method can be used to control the shrinkage behavior in the LTCC thickness range from 1.0 mm to 5.0 mm.

Conclusions

In this study, the L-PAS method was suggested and the edge curvature problem was investigated. The symmetric structure of an entire sandwich 'alumina/many LTCC/alumina' was determined for the L-PAS method. As the load increased, the shrinkage along the x-y directions decreased while both the shrinkage along the z direction and edge curvature increased. Above an 800 g load, deformation occurred. As the LTCC thickness increased, the shrinkage along the x-y directions increased while both the shrinkage along the z direction and the edge curvature decreased. The L-PAS method can be used to control the shrinkage behavior in the LTCC thickness range from 1.0 mm to 5.0 mm. A zero-shrinkage substrate which has a shrinkage along the x-y directions below 0.2% and that along the z direction of 37% when sintered at 900 °C for 30 minutes with the an LTCC thickness of 2.9 mm and a load of 800 g. The edge curvature was measured as 10500 μm and the sintered density was 3.02 g/cm².

References

1. Y. Higuchi, Y. Sugimoto, J. Harada and H. Tamura, J. Eur. Ceram. Soc., 27[8] (2007) 2785-2788.
2. M. Matters-Kammerer, U. Mackens, K. Reimann, R. Pietig, D. Hennings, B. Schreinemacher, R. Mauczok, S. Gruhlke and C. Martiny, Microelectronics & Reliability, 46[1] (2006) 134-143.
3. J.H. You, D.H. Yeo, H.S. Shin, J.H. Kim and H.G. Yoon, J. Electroceramics, 23 (2009) 367-371.
4. W.A. Vitrio, R.L. Brown and U.S. Patent No. 4656552 (1987).
5. F. Lautzenhiser and E. Amaya, Am. Ceram. Soc. Bull., 81 (2002) 27-33.
6. K.R. Mikeska, D.T. Schaefer and R.H. Jensen, U.S. Patent No. 5085720, (1992).
7. W.A. Vitrio and R.L. Brown, U. S. Patent No. 4656552, (1987).
8. C.B. Wang, K.W. Hang and C.R.S. Needes, U.S. Patent No. 6776861, (2004).
9. A. Mohanaram, S.H. Lee, G.L. Messing and D.J. Green, J. Am. Ceram. Soc., 89[6] (2006) 1923-1929.
10. M.F. Wtzel, R.Y. Ballester, J.B.C. Meira, R.G. Limab and R.R. Braga, Dent. Mater., 23 (2007) 204-210.